ISSN: 1410-8917
e-ISSN: 2597-9914

Jurnal Kimia Sains dan Aplikasi 25 (5) (2022): 169–178

Jurnal Kimia Sains dan Aplikasi
Journal of Scientific and Applied Chemistry

Journal homepage: http://ejournal.undip.ac.id/index.php/ksa

Molecular Docking Study of IPBCC.08.610 Glucose Oxidase Mutant for Increasing Gluconic Acid Production

Shobiroh Nuur'Alimah [a], Tony Ibnu Sumaryada [b], Waras Nurcholis [a,c], Laksmi Ambarsari [a,*]

[a] Department of Biochemistry, Faculty of Mathematics and Natural Sciences, IPB University, Bogor, Indonesia
[b] Department of Physics, Faculty of Mathematics and Natural Sciences, IPB University, Bogor, Indonesia
[c] Tropical Biopharmaca Research Center, IPB University, Bogor, Indonesia

*Corresponding author: laksmi@apps.ipb.ac.id

https://doi.org/10.14710/jksa.25.5.169-178

Article Info

Article history:

Received: 25th February 2022
Revised: 30th April 2022
Accepted: 18th May 2022
Online: 31st May 2022

Keywords:
gluconic acid; glucose oxidase; mutation; molecular docking

Abstract

Glucose oxidase (GOD) is an oxidoreductase enzyme that catalyzes the oxidation of glucose to gluconolactone and hydrogen peroxide. Then, gluconolactone will be hydrolyzed to gluconic acid. The wide application of gluconic acid in various industries has increased production demand. However, glucose concentrations higher than 40% (w/w) inhibited the conversion of glucose to gluconic acid due to a decrease in the oxygen solubility concentration at pH 6, 30°C, and 1 bar pressure. Therefore, decreasing the value of Km is predicted to reduce saturation and enhance gluconic acid production. This study aimed to analyze the interaction between the IPBCC.08.610 GOD mutant with β-D-Glucose in improving gluconic acid production by decreasing the Km value. Mutations were performed in silico using Chimera and then docked using AutoDock Vina. The mutations resulted in distinct ligand poses in the binding pocket, different -OH conformations of the ligands, and changes in the T554M/D578P mutant's hydrophobicity index (554 mutated from threonine to methionine, and 578 mutated from aspartate to proline), and decreased ΔG and Km values in the H559D mutant (559 mutated from histidine to aspartate), D578P and T554M/D578P. This decrease might strengthen the ligand-receptor interaction, increasing gluconic acid production. The H559D was the best mutant to increase production based on the ΔG, Km value, and stability due to the addition of hydrogen bonds.

1. Introduction

Glucose oxidase (GOD) is an oxidoreductase enzyme consisting of two identical subunits measuring 80 kDa [1]. This enzyme catalyzes the oxidation of β-D-glucose to β-D-glucono-1,5-lactone and H_2O_2 using molecular oxygen as an electron acceptor. Then β-D-glucono-1,5-lactone will be hydrolyzed by lactonase into gluconic acid. However, the presence of these enzymes is unnecessary because the hydrolysis step can occur spontaneously [2]. GOD can be produced by various organisms, such as bacteria, plants, animals, and fungi; however, GOD from fungi has a broader spectrum of applications. The fungi used to produce GOD enzymes are mainly from *Aspergillus* and *Penicillium* [3]. The GOD derived from *Aspergillus niger* is classified as an intracellular enzyme and is the most widely commercialized due to its stability in a wide pH and temperature range (pH 4–7 and temperature of 20–50°C) [4].

GOD can be applied as a biosensor in measuring blood sugar levels, detecting fruit ripeness [5, 6], and a micro-fuel cell [7]. The H_2O_2 produced by GOD is used as a bleach in the textile industry. Furthermore, the resulting H_2O_2 can also act as an antibacterial agent [8, 9]. Another GOD product—gluconic acid—also has many benefits and potential applications in various industries, including beverage, food, animal feed, pharmaceutical, textile, and construction [10]. According to Ramachandran *et al.* [11], some of the benefits of gluconic acid include preventing milkstone formation during the heating of milk and iron

deposition in textiles, cleaning aluminum cans, food preservatives, and nutritional additives in animal feed.

The widespread use of gluconic acid has increased the production demands. According to Ramachandran *et al.* [11], worldwide gluconic acid production reaches 100,000 tons/year. Research by Tomotani *et al.* [12] regarding gluconic acid production from glucose oxidation by glucose oxidase using a membrane bioreactor resulted in a GOD activity value of 75.2×10^{-3} U/mL for Vmax and 29 mM for Km. The amount of gluconic acid produced by GOD dramatically depends on the amount of substrate and dissolved oxygen present. Glucose concentration higher than 40% (w/w) can inhibit the conversion of glucose into gluconic acid due to a decrease in oxygen solubility concentration with increasing solids concentration, causing it to become saturated. This occurs at pH 6, temperature 30°C, and 1 bar pressure [13, 14]. Therefore, decreasing the Km value is expected to reduce saturation and increase gluconic acid production. One practical approach that can be done to minimize the Km value is by mutating the catalytic residue or residue that can increase enzyme activity.

Mutations in this study were conducted on several residues in the GOD gene encoding IPBCC.08.610 derived from local isolates of *Aspergillus niger* isolated by Khanza [15], and their nucleotide sequences were obtained from NCBI with accession code MH593586.1. These residues were T554, H559, and D578 (Figure 1). The mutation on T554 residue was based on Marín-Navarro *et al.* [16], which mutated the T554 to M554 (T554M) residue of GOD 1CF3, causing a 40% increase in thermal stability compared to wild-type due to the formation of sulfur-pi interactions in the mutant. Meanwhile, H559 residue is the enzyme's catalytic residue [17], and D578 residue in IPBCC.08.610 GOD is the main element stabilizing the C-terminus by forming a salt bridge with R545 and R537 [18].

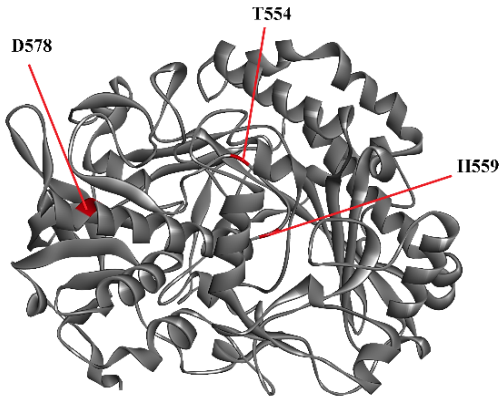

Figure 1. Mutated residues of IPBCC.08.610 GOD

Research on mutations of IPBCC.08.610 GOD has been studied by Puspita *et al.* [19] on H516 to H516R and H516D residues for fuel cells. The study resulted in the affinity energy value (ΔG) of -6.5 kcal/mol and the Km value of 17.187 M for the wild-type and the H516R mutant. In contrast, ΔG and the Km value of the H516D mutant were 6.2 kcal/mol and 28.517 M, respectively. These findings revealed that in the H516D mutation, the ΔG and Km values increased, improving the potential for GOD as a fuel cell. Meanwhile, no research on IPBCC.08.610 GOD mutations to increase gluconic acid production has been conducted. Therefore, this study aimed to analyze in silico interaction between T554M, H559D, D578P, and T554M/D578P mutants of IPBCC.08.610 GOD with β-D-Glucose as a ligand in order to increase gluconic acid production by decreasing the Km value.

2. Methodology

2.1. Equipment and Materials

A laptop with specifications of processor Intel® Core™ i7-8550UU equipped with 16 GB of RAM, Microsoft Windows™ 10 64-Bit operating system. The software used includes AutoDockTools 1.5.6, YASARA, Discovery Studio Visualizer 3.5 Client, Chimera 1.14, BioEdit, PyMOL, LigPlot+, Open Babel, PROCHECK https://saves.mbi.ucla.edu/ dan SWISS-MODEL https://swissmodel.expasy.org/.

The materials in this study consisted of the nucleotide sequence of the IPBCC.08.610 GOD enzyme obtained from the NCBI online database https://www.ncbi.nlm.nih.gov/ with accession code MH593586.1, the 3D structure of the ICF3 receptor downloaded from RCSB database https://www.rcsb.org/ and 3D β-D-Glucose ligand structure obtained from PubChem database https://pubchem.ncbi.nlm.nih.gov/.

2.2. Ligand Preparation

The ligand employed in this study was β-D-glucose. The 3D ligand structure was downloaded from the PubChem website in *.sdf file format and converted into *.pdb file format, then prepared using Discovery Studio Visualizer 3.5 Client and saved as ligand.pdb. Ligand preparation involved adding hydrogen atoms and removing other structures from the ligand.

2.3. Receptor Preparation

The IPBCC.08.610 GOD receptor was downloaded from the NCBI online database and stored in *.fasta file format. The data obtained was converted into a 3D structure in *.pdb file format using the web-based software SWISS-MODEL [20] and saved as receptor.pdb. The structure of the 1CF3 receptor was also downloaded from the RCSB online database in *.pdb file format. All unwanted water, residues, and natural ligands were removed from the receptor before hydrogen atoms were attached using the Discovery Studio Visualizer 3.5 Client [21] and saved as *.pdb file format.

2.4. Receptor Mutation

This procedure cited the studies of [20, 22]. The receptor file in the prepared *.pdb file format was opened using Chimera 1.14 [23]. The mutation was done by highlighting the residue to be mutated. The mutation with the highest probability of not colliding with other atoms was chosen. The resulting receptor was then saved in *.pdb file format. The T554 residue was mutated into M554, the H559 residue into D559, the D578 residue into P578, and the double mutant T554M/D578P. The receptors were minimized using YASARA [24].

2.5. Mutant Structure Analysis

The structure of the mutant receptor was evaluated using the Ramachandran plot on the PROCHECK web server [25] and compared with the original receptor analyzed by the same method [26]. Using OpenBabel, the codon level structure was investigated by converting the data format from *.pdb to *.fasta [27]. Nucleotide sequence changes can be analyzed using reverse translation with BioEdit software [28].

2.6. The Preparation of Mutant Receptor, Ligand, and Molecular Docking Parameters

This procedure referred to a study from [29]. Both mutated and wild-type receptors were opened using AutoDockTools 1.5.6 [30]. The docking parameters must be validated before the molecular docking simulation by determining the grid box size that generates the highest negative affinity energy and the smallest RMSD average value, both at the lower bound (LB) and the upper bound (UB). Molecular docking was conducted at positions 45.535, 12.575, and 57.350 (x, y, z) with grid box size 26.24 and 28 (x, y, z) and spacing of 0.453.

2.7. Molecular Docking Simulation

Molecular docking performed was oriented docking or targeted docking with the help of Command Prompt (CMD) [29]. Receptors, ligands, and AutoDock Vina were placed in the same folder. The docking command was written in CMD. The procedure was repeated 20 times using the num_modes command, pairing the pre-prepared ligands with each prepared receptor (wild-type or mutant). The docking results were saved in the working folder as log.txt and output.pdbqt file format. The highest ΔG value was attained in the first mode.

2.8. Analysis of Ligand and Receptor Interaction

The output.pdbqt file generated by molecular docking and the receptor file in *.pdbqt file format were visualized using Discovery Studio Visualizer 3.5 Client [29]. The first mode of output.pdbqt was selected and copied into the receptor file, then saved in *.pdb file format. The molecular docking results were analyzed for ligand-receptor interactions using LigPlot+ [31], PyMOL [32], and Discovery Studio Visualizer 3.5 Client. The analysis results were in the form of 2D and 3D images. The Michaelis-Menten constant (Km) was calculated from the ΔG of the ligand, using the equation $\Delta G = -RT \ln Km$ [33].

3. Results and Discussion

3.1. IPBCC.08.610 GOD Structure

The 3D structure of the IPBCC.08.610 GOD sequence was obtained through a homology modeling process using the SWISS-MODEL web-server. Homology modeling is a procedure for constructing a 3D model of a target primary sequence based on an experimentally known sequence or structure (template) [34]. The 1CF3 template was applied for modeling. According to Maulana [18], 1CF3 has superior model quality based on MolProbity and stereochemical properties compared to 5NIT. The obtained 3D structure consisted of 581 residues of the glucose oxidase enzyme with Flavin-Adenine Dinucleotide (FAD) as a ligand (Figure 2). This receptor's residue sequence initiated at residue 25 and ended at 605, providing 22 more residues than the template. These 22 residues are signal peptide sequences that are not integrated as components of the tertiary structure [18].

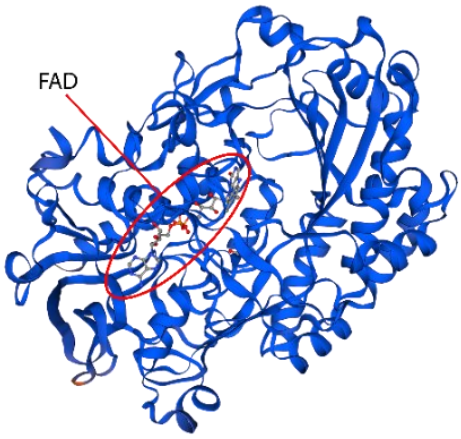

Figure 2. 3D structure of IPBCC.08.610 GOD modeling results

The homology modeling generates sequence identity, MolProbity, GMQE, and QMEAN values. As a result, the sequence identity value was 97.08%. Sequence identity indicates the accuracy of the sequence between the target and the template. According to Raiyn and Rayan [35], the model is considered good if the sequence identity is greater than 60%. The greater the sequence identity between the target and the template, the closer the model is to the real one. The modeling also produced a MolProbity value of 0.91. MolProbity performed contact analysis between all atoms, Ramachandran plot, and rotamer distribution (side chain) [36]. A lower MolProbity value indicates a higher structural quality [37].

Meanwhile, the resulting GMQE and QMEAN values were 0.96 and -0.09. GMQE (Global Model Quality Estimation) and QMEAN (Quality Model Energy Analysis) are expressed as numbers between zero and one; higher numbers indicate higher quality and similarity to templates [38, 39]. However, a model with a QMEAN score of 4.0 or less is deemed low-quality [40], meaning that the modeling has a significant degree of resemblance to the protein sequence of the 1CF3 template.

The structural quality of the receptor can be determined using the Ramachandran plot. This plot is a coordinate or diagram formed from the distribution of amino acid residues that arrange a protein at two types of angles; the phi (ϕ) as the x-axis and the psi (ψ) as the y-axis [41]. The Ramachandran plot is divided into four quadrants, including the most favorite regions (quadrant I) in red, additional allowed regions (quadrant II) in yellow, generously allowed regions (quadrant III) in pale yellow, and disallowed regions (quadrant IV) in white. The analysis results showed that wild-type receptors had 89.4% residues in quadrant I, 10.4% residues in quadrant II, 0.2% residues in quadrant III, and 0% residues in quadrant IV (Figure 3). A good quality model or structure is expected to have more than 80% residues in the most favored region and less than 1% non-

glycine residues in disallowed regions [42]. The 3D model of the wild-type receptor that has been made has good quality because there are more than 80% residues in the most favored region.

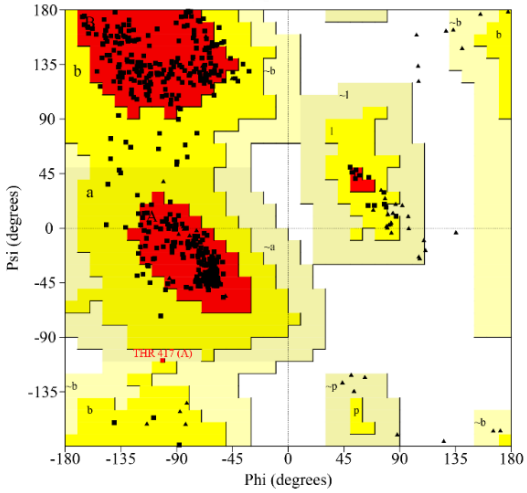

Figure 3. Ramachandran plot of modeled receptors (wild-type)

3.2. Residual Mutations and Changes in Codon Level

The IPBCC.08.610 GOD was mutated four times by point mutations at residues T554, H559, D578, and double mutant T554/D578 (Table 1). A point mutation is the alteration of a single base pair into another. This type of mutation is classified as non-conservative substitution, changing mutation into residues that have different properties [43]. According to Clark *et al.* [44], non-conservative substitutions result in significant changes to the protein. The success of the mutation method can be determined by examining the codon sequence and protein structure using the Ramachandran plot.

Table 1. Changes in codon levels due to mutations

No	Mutant enzyme	Amino acid residue			Codon	
		Before mutation	After mutation	Codon position	Before mutation	After mutation
1	T554M	T554	M554	1654–1656	ACC	ATG
2	H559D	H559	D559	1669–1671	CAT	GAT
3	D578P	D578	P578	1726–1728	GAT	CCG
4	T554M/ D578P	T554 D578	M554 P578	1654–1656 1726–1728	ACC GAT	ATG CCG

Changes in the codon sequence can be analyzed using the reverse translate command in the BioEdit software. The codon of the receptor was encoded by three nucleotides. The T554 residue mutated from the polar neutral threonine (T) (ACC) to the non-polar methionine (M) (ATG) at positions 1654–1656 in the nucleotide sequence. The H559 residue at positions 1669–1671 altered from the positive polar histidine (H) (CAT) to the negative polar aspartate (D) (GAT). The D578 residue mutated from a negative polar aspartate (D) (GAT) to a non-polar proline (P) (CCG) in the nucleotide sequence at 1726–1728. The double mutant T554M/D578P combines the two previously mentioned mutations (Table 1). Meanwhile, the quality of the receptor resulting from the mutation can also be observed using the Ramachandran plot. All mutant receptors had the same Ramachandran plot results as the modeled receptors (wild-type) (Figure 3).

3.2.1. Molecular Docking and Mutant Structural Changes

Molecular docking in this study was categorized as oriented docking or targeted docking because the grid box was created based on the receptor's active site, which Meyer studied [45]. The active sites include Tyr 68, Thr 110, Glu 412, Phe 414, Arg 512, Asn 514, His 516, His 559 for hydrogen-bonded residues, Asp 424, Tyr 515, and Trp 426 for amino acid residues having hydrophobic bonds. Meanwhile, residues that play a role in the enzyme's catalytic site are Glu 412, His 516, and His 559 [17]. Molecular docking was performed on the 3D structure of the IPBCC.08.610 GOD in the form of Apoenzyme (without FAD) as a receptor (both wild and mutant types), the structure of glucose oxidase 1CF3 as a comparison receptor, and β-D-glucose as a ligand.

Aside from preparation, the docking parameters and methods were validated 20 times with the RMSD parameter and ΔG value (Supplementary 1). The smallest average RMSD values at both the lower bound (LB) and the upper bound (UB) of wild-type receptor were employed for docking. According to Rollando [46], the docking method will be more effective if the RMSD value is less than 2.5 Å. Meanwhile, the ΔG with the most negative value was employed since it indicated a strong ligand affinity for the active region of the receptor [47]. The docking was accomplished at 45.535, 12.575, and 57.350 (x, y, z) with grid box sizes of 26, 24, and 28 (x, y, z) and grid spacing of 0.453. The energy of both wild-type and mutant receptors was minimized by YASARA [24], finding the lowest energy conformation of a molecule.

The docking results were compared to the binding site of IPBCC.08.610 GOD (Figure 4) and ICF3 as Binding Similarity Site (%BSS) from Meyer's research [45] (Table 2). The analysis results showed that the wild-type receptor had ten identical residues to the eleven residues of the enzyme's active site, resulting in a %BSS value of 90.91%. The H559D and D578P mutations had the same %BSS value of 81.82%, which indicated that 9 out of 11 residues match the template, while the double mutant T554M/D578P produced the smallest %BSS value of 18.20%, with 2 of 11 residues matching.

The comparison results also showed that His 516 residues were present in all receptors (wild-type, comparison, and mutant). All receptors except those with double mutant T554M/D578P had His 559 residues; however, the Glu 421 residues in wild-type, the 1CF3, and the mutant receptor were undiscovered. The absence of these residues can be caused because Glu 412 does not bind or directly interact with the ligand, but hydrogen bonds with His 559 [19]. Another reason is that some Glu 412 residues are buried within the enzyme, in contrast to His 516 residues which are more flexible, solvent-exposed, and visible from the surface [48]. The difference in %BSS values indicates that the mutated residue affects the binding site.

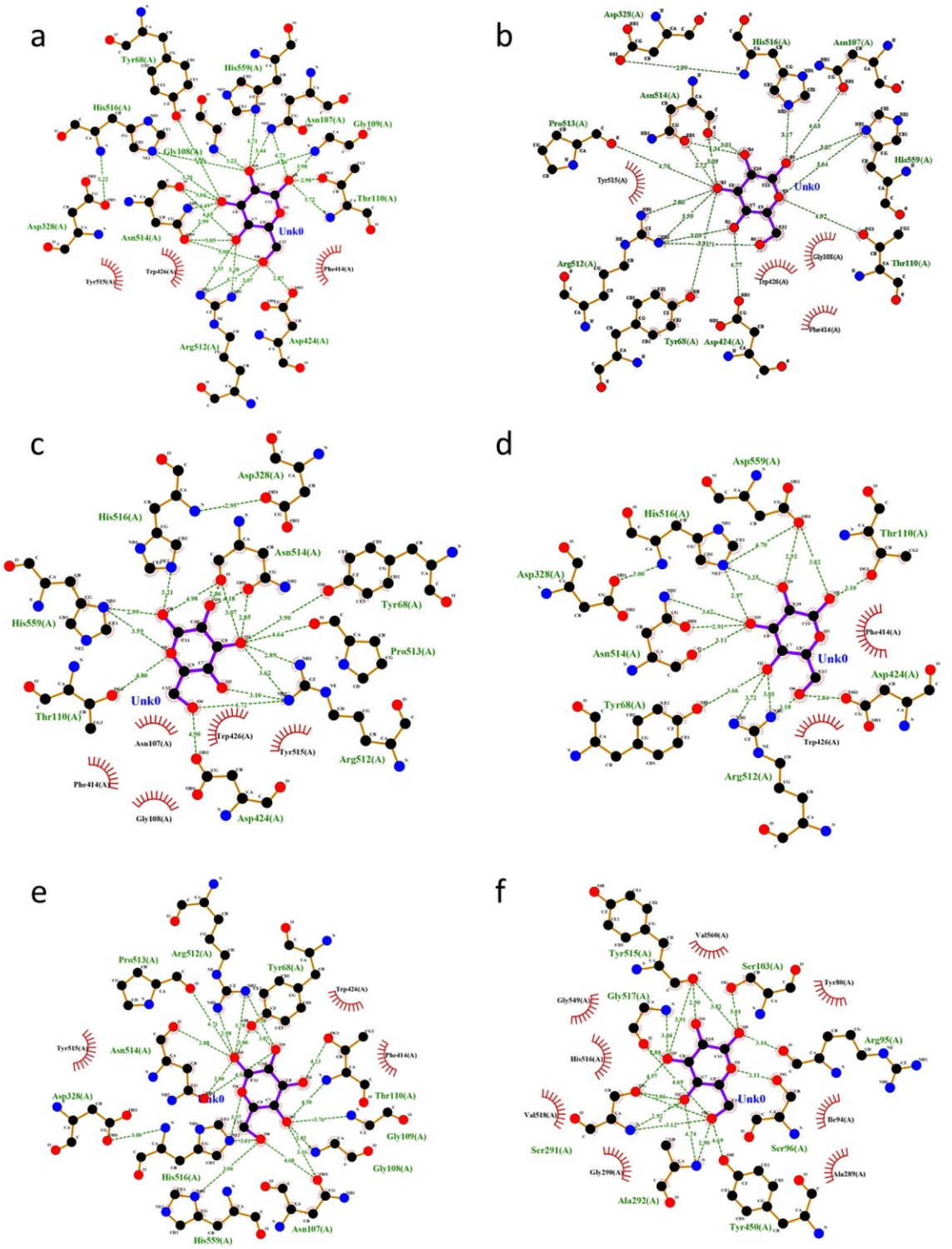

Figure 4. 2D visualization of the active site of glucose oxidase binding with β-D-glucose as a ligand (a) 1CF3 (b) wild-type (c) T554M (d) H559D (e) D578P (f) T554M/D578P

In addition to %BSS, the entire docked receptor was also analyzed for its hydrophobicity index or scale with the Discovery Studio Visualizer 3.5 Client at the binding site. This hydrophobicity scale is based on the Kyte-Doolittle Scale, widely used to detect hydrophobic regions in proteins. Hydrophobicity is a physical property of molecules that repels water. The hydrophobicity index is described on a scale of +3.00 (brown) to −3.00 (blue)—the more positive the value, the more hydrophobic the molecule [49]. According to the visualization data, the ICF3, wild-type, and all mutant receptors showed low hydrophobicity or were even likely to be negative, except for the receptor with the double mutant T554M/D578P, indicated in blue at the binding site. In contrast, the double mutant T554M/D578P receptor exhibited a neutral hydrophobicity index (0.0) marked in white at the binding site (Figure 5).

Table 2. Comparison of docked receptor interactions with 1CF3

Receptors	Amino acid residue		BSS (%)
	Hydrogen bond	Hydrophobic bond	
1CF3 (Meyer *et al.* [45])	Tyr 68, Thr 110, Glu 412, Phe 414, Arg 512, Asn 514, His 516, His 559	Asp 424, Tyr 515, Trp 426	100.00%
1CF3	**Tyr 68**, Gly 108, Gly 109, **Thr 110,** Asp 328, **Asp 424, Arg 512, Asn 514, His 516, His 559**	Asn 107, **Phe 414, Trp 426, Tyr 515**	90.91%
Wild-type	**Tyr 68**, Asn 107, **Thr 110**, Asp 328, **Asp 424, Arg 512**, Pro 513, **Asn 514, His 516, His 559**	Gly 108, **Phe 414, Trp 426, Tyr 515**	90.91%
T554M	**Tyr 68, Thr 110**, Asp 328, **Asp 424, Arg 512**, Pro 513, **Asn 514, His 516, His 559**	Asn 107, Gly 108, **Phe 414, Trp 426, Tyr 515**	90.91%
H559D	**Tyr 68, Thr 110,** Asp 328, **Asp 424, Arg 512, Asn 514, His 516,** *Asp* **559**	**Phe 414, Trp 426**	81.82%
D578P	**Tyr 68**, Asn 107, Gly 108, Gly 109, **Thr 110**, Asp 328, **Arg 512**, Pro 513, **Asn 514, His 516, His 559**	**Phe 414, Trp 426, Tyr 515**	81.82%
T554M/D578P	Arg 95, Ser 96, Ser 103, Ser 291, Ser 292, Tyr 450, **Tyr 515**, Gly 517	Tyr 80, Ile 94, Ala 289, Gly 290, **His 516,** Val 518, Gly 549, Val 560	18.20%

Note: The writing in bold is the same residue between the docked receptors and the receptors from previous studies

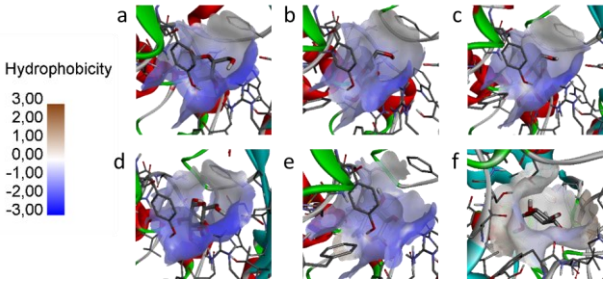

Figure 5. Hydrophobicity of IPBCC.08610 GOD receptors (a) 1CF3 (b) wild-type (c) T554M (d) H559D (e) D578P (f) T554M/D578P

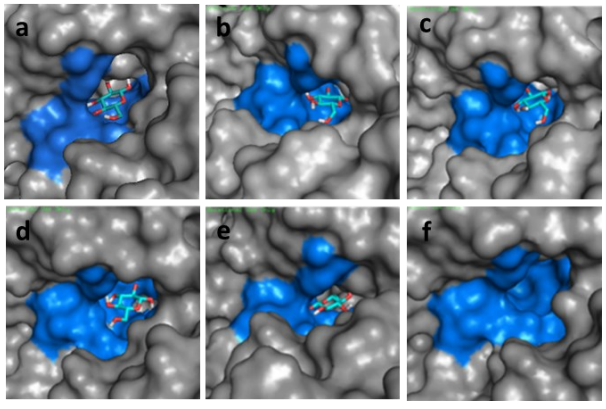

Figure 6. Visualization of the binding pocket resulting from the binding of the IPBCC.08.610 GOD receptor with the β-D-glucose ligand. The blue color shows the active site of the receptors (a) 1CF3 (b) wild-type (c) T554M (d) H559D (e) D578P (f) T554M/D578P

The mutation also causes differences in the binding pocket, which may be visualized using PyMOL. The blue color indicates the receptor's active site, while the molecule in the stick-shaped pocket is an β-D-glucose ligand (Figure 6). According to the visualization results, the binding pocket on the receptor differs, especially at the location of the binding ligand (Figure 6). Ligands for both the wild-type and mutant receptors are seen on the surface of the binding pocket; except for the double mutant T554M/D578P, the ligand is invisible on the surface. In addition to differences in ligand location, mutations also influence the entire -OH conformation of the β-D-glucose ligand at all receptors (Figure 7).

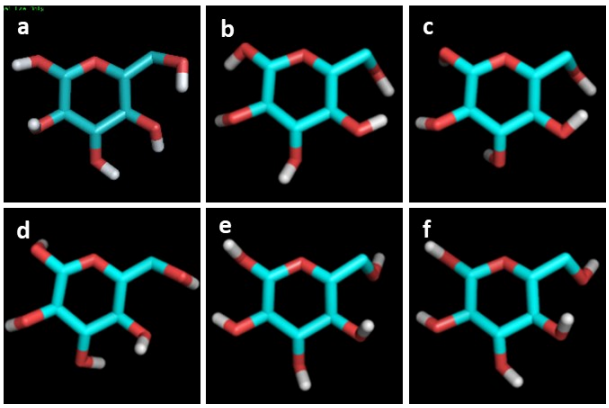

Figure 7. Visualization of β-D-glucose ligand molecule binding to IPBCC.08.610 GOD receptors (a) 1CF3 (b) wild-type (c) T554M (d) H559D (e) D578P (f) T554M/D578P

Aside from hydrophobicity, binding site, and binding pocket, the mutated residues in mutant receptors were analyzed and visualized. The T554M receptor mutated from the Thr 554 (T554) residue to Met 554 (M554). This causes the hydrogen bond between the Trp 122 and Thr 554 residues to break, forming a new interaction between the Met 554 residue and the Phe 126 ring center (Figure 8). The interaction created between the M554 mutant and F126 is a pi-sulfur bond, which involves the interaction of the sulfur atom of the methionine residue with the aromatic group of the phenylalanine residue [50]. The interaction of sulfur with the aromatic ring formed an intermolecular distance of 4.8 with a 40.5° angle between the sulfur atom and normal vector to the plane defined by the aromatic ring at its center.

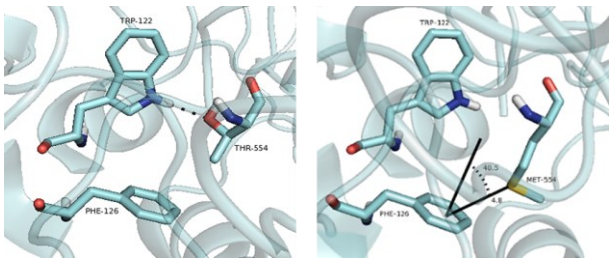

Figure 8. 3D visualization of IPBCC.08.610 receptor mutation from wild-type T554 residues (left) to M554 mutant (right)

Meanwhile, according to Marín-Navarro *et al.* [16], who mutated the similar T554M residue of glucose oxidase 1CF3, the intermolecular distance between the sulfur and the center of the aromatic ring was 5.5, with angel ranging from 30 to 60° between the sulfur atom and the normal vector to the plane defined by the aromatic ring at the center of the ring (Figure 9). The difference between the results and the literature is due to the different conformations of the mutated sulfur atom compared to the sulfur atom of methionine residue in the

literature. However, the angle formed at the T554M mutant of IPBCC.08.610 GOD receptor follows the literature.

The hydrogen bond breaking and the formation of sulfur-pi interactions can improve the stability of the enzyme. This is because the sulfur-pi interaction produces energy of 4.2–12.6 kJ/mol, comparable to the stabilization produced by the salt bridge (4.2–13.4 kJ/mol) and higher than hydrogen bonding (1.3–6.3 kJ/mol) [50]. However, there was no difference in the value of ΔG and Km compared to the wild-type.

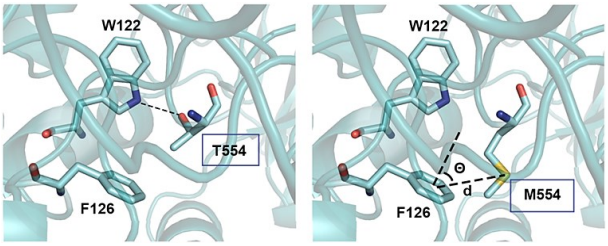

Figure 9. Visualization of residue T554M of ICF3 mutant receptor structure [16]

The H559D mutant receptor mutated from His 559 (H559) residue to Asp 559 (D559) residue, which caused the addition of hydrogen bonds at D559 and H516 residues. The interaction between H559 residue of the wild type and ligand formed two hydrogen bonds with distances of 3.07 Å and 3.64 Å. The D559 mutant formed three hydrogen bonds, two of which bind to a ligand at distances of 2.92 Å and 3.02 Å, one to a H516 residue at a distance of 4.70 Å (Figure 10).

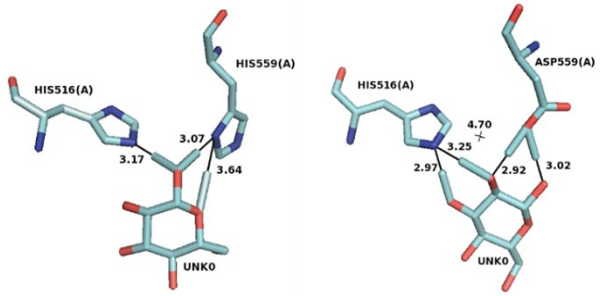

Figure 10. 3D visualization of the IPBCC.08.610 receptor mutation from a wild-type H559 residue (left) to a D559 mutant (right)

The ΔG will become increasingly negative as the number of hydrogen bonds increases [51]. In addition, the hydrogen bond distance formed after the mutation is shorter than the wild-type. After mutations, the addition and shortening of hydrogen bonds strengthen ligand-receptor interactions and enhance enzyme stability. According to Kumar *et al.* [52], the amount of hydrogen bonds is one factor that can influence the enzyme's stability.

Another mutant receptor, D578P, which mutated from Asp 578 (D578) to Pro 578 (P578) residues, caused the cleavage of the salt bridge between Asp 578 (D578) and Arg 545 (R545) residues on wild-type (Figure 11). According to Maulana [18], due to molecular dynamics, the D578 residue on the wild-type receptor has a salt bridge with R545 and R537 residues. However, based on the results of docking and visualization, the salt bridge was only formed at the R545 residue on the wild-type receptor. In contrast, no salt bridge was detected in both residues in the mutant.

The difference in wild-type results between molecular dynamics and docking is related to a methodological difference. Molecular docking is rigid, while molecular dynamics allow molecules to move around and develop new interactions. In addition, the values of ΔG and Km decreased in mutants compared to the wild-type. This agrees with Mhaindarkar *et al.* [53], who observed that breaking the salt bridge decreases the value of Km and the enzyme stability. Meanwhile, the mutant receptor with double mutant T554M/D578P underwent the same events as the T554M mutant receptor and the D578P mutant receptor.

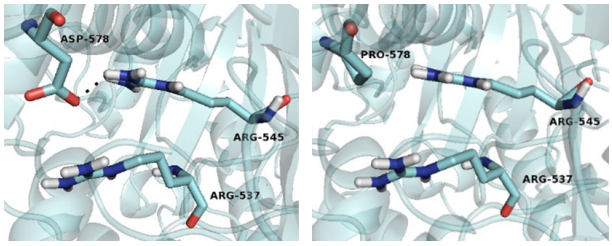

Figure 11. 3D visualization of the IPBCC.08.610 receptor mutation from a wild-type D578 residue (left) to a mutant P578 mutant (right)

3.2.2. Energy Affinity and Michaelis-Menten Constant

As a result of molecular docking, a "log" file including the affinity energy and RMSD was produced. Affinity Energy is defined as the amount of energy required by the ligand to bind to the receptor. The energy affinity (ΔG) can also be utilized to analyze the ligand-receptor interaction's stability [47]. The lowest ΔG with an RSMD value of 0.000 resulting from molecular docking can be applied to calculate the Michaelis-Menten constant (Km). The constant is defined as substrate concentration that causes the reaction rate to be half of its maximum rate (Vmax) [54].

The ΔG and Km values of the ICF3, wild-type, and the T554M mutant receptor were -5.7 kcal/mol and 66.353 M, respectively. The ΔG and Km values of the H559D mutant receptor and the T554M/D578P mutant were -5.9 kcal/mol and 47.344 M, respectively. Meanwhile, the D578P mutant receptor produces ΔG of -5.8 kcal/mol and a Km value of 56.048 M (Table 3). The results showed that the H559D, D578P, and T554M/D578P mutants had changes in ΔG values accompanied by a decrease in Km values. According to Bassingthwaighte and Chinn [54], the ΔG value is proportional to the Km value. The more negative the ΔG, the smaller the value of Km. A more negative ΔG indicates a higher ligand affinity for the receptor's active site [47], has a spontaneous and stable interaction, and stronger ligand-receptor binding [29, 55].

Table 3. Molecular docking interactions

Ligand	Receptor	Energy affinity (ΔG) (kcal/mol)	Michaelis Constant-Menten (Km) (μM)
β-D-glucose	1CF3	-5.7	66.353
	Wild-type	-5.7	66.353
	T554M	-5.7	66.353
	H559D	-5.9	47.344
	D578P	-5.8	56.048
	T554M/D578P	-5.9	47.344

These results indicate that the mutation did not significantly differ in the glucose binding reaction with the T554M mutant receptor because the resulting Km value was the same as that of the wild-type receptor of the IPBCC.08.610 GOD enzyme and 1CF3. In contrast, the other three mutant receptors (H559D, D578P, and T554M/D578P) exhibited lower Km values than the wild-type. This indicates that the mutation affects glucose binding to the receptor, and the three mutants can enhance gluconic acid production.

4. Conclusion

The ΔG and Km values of the T554M mutant were unaffected by mutation, whereas both values were reduced in the H559D, D578P, and T554M/D578P mutants. Reduced ΔG and Km values of the three mutants can strengthen the binding of glucose as a ligand with the receptor, enhancing gluconic acid production. The H559D mutant was the best mutant for increasing the production based on the ΔG, Km value, and high stability due to the addition of hydrogen bonds.

References

[1] Muhammad Anjum Zia, Ayesha Riaz, Samreen Rasul, Rao Zahid Abbas, Evaluation of antimicrobial activity of glucose oxidase from *Aspergillus niger* EBL-A and *Penicillium notatum*, *Brazilian Archives of Biology and Technology*, 56, 6, (2013), 956-961 https://doi.org/10.1590/S1516-89132013005000010

[2] Shweta V. Bhat, B.R. Swathi, Maria Rosy, M. Govindappa, Isolation and charecterization of glucose oxidase (GOD) from *Aspergillus flavus* and *Penicillium* sp., *International Journal of Current Microbiology and Applied Sciences*, 2, 6, (2013), 153-161

[3] Manish K. Dubey, Andleeb Zehra, Mohd Aamir, Mukesh Meena, Laxmi Ahirwal, Siddhartha Singh, Shruti Shukla, Ram S. Upadhyay, Ruben Bueno-Mari, Vivek K. Bajpai, Improvement strategies, cost effective production, and potential applications of fungal glucose oxidase (GOD): current updates, *Frontiers in Microbiology*, 8, 1032, (2017), 1-22 https://doi.org/10.3389/fmicb.2017.01032

[4] Chun Ming Wong, Kwun Hei Wong, Xiao Dong Chen, Glucose oxidase: natural occurrence, function, properties and industrial applications, *Applied Microbiology and Biotechnology*, 78, 6, (2008), 927-938 https://doi.org/10.1007/s00253-008-1407-4

[5] Hui-Chen Wang, An-Rong Lee, Recent developments in blood glucose sensors, *Journal of Food and Drug Analysis*, 23, 2, (2015), 191-200 https://doi.org/10.1016/j.jfda.2014.12.001

[6] Andi Mulyadi, Biosensor Glukosa Termodifikasi Nanoserat Polianilin dari Glukosa Oksidase *Aspergillus niger* IPBCC. 08.610 sebagai Detektor Kematangan Buah, *Master Thesis*, Department of Biochemistry, IPB University, Bogor, 2019

[7] Laksmi Ambarsari, Akhiruddin Maddu, Titi Rohmayanti, Waras Nurcholis, An optimized glucose biosensor as a potential micro-fuel cell, *Rasayan Journal of Chemistry*, 11, 1, (2018), 32-36 http://dx.doi.org/10.7324/RJC.2018.1111981

[8] José C. Soares, Patrícia R. Moreira, A. Catarina Queiroga, José Morgado, F. Xavier Malcata, Manuela E. Pintado, Application of immobilized enzyme technologies for the textile industry: a review, *Biocatalysis and Biotransformation*, 29, 6, (2011), 223-237 https://doi.org/10.3109/10242422.2011.635301

[9] MR Hakim, T. Sumaryada, L. Ambarsari, Antibacterial based on IPBCC. 08.610 glucose oxidase against UDP-N-acetyl glucosamine enolpyruvyl transferase and elongation factor G enzymes *in silico*, *IOP Conference Series: Earth and Environmental Science*, 2019 https://doi.org/10.1088/1755-1315/299/1/012035

[10] Qingxuan Mu, Yinglu Cui, Meirong Hu, Yong Tao, Bian Wu, Thermostability improvement of the glucose oxidase from Aspergillus niger for efficient gluconic acid production via computational design, *International Journal of Biological Macromolecules*, 136, (2019), 1060-1068 https://doi.org/10.1016/j.ijbiomac.2019.06.094

[11] Sumitra Ramachandran, Pierre Fontanille, Ashok Pandey, Christian Larroche, Gluconic acid: properties, applications and microbial production, *Food Technology & Biotechnology*, 44, 2, (2006), 185-195

[12] Ester Junko Tomotani, Luiz Carlos Martins das Neves, Michele Vitolo, Oxidation of glucose to gluconic acid by glucose oxidase in a membrane bioreactor, *Applied Biochemistry and Biotechnology*, 121, 1, (2005), 149-162 https://doi.org/10.1385/ABAB:121:1-3:0149

[13] Oreste J. Lantero, Jayarama K. Shetty, *Process for the preparation of gluconic acid and gluconic acid produced thereby*, Google Patents, United States, 2005

[14] Savas Anastassiadis, Igor G. Morgunov, Gluconic acid production, *Recent Patents on Biotechnology*, 1, 2, (2007), 167-180 http://dx.doi.org/10.2174/187220807780809472

[15] Annisa Dhiya Athiyyah Khanza, Karakterisasi dan Kloning Gen Penyandi Glukosa Oksidase (GGOx) dari Aspergillus niger IPBCC 08.610, *Undergraduate Thesis*, Department of Biochemistry, IPB University, Bogor, 2016

[16] Julia Marín-Navarro, Nicole Roupain, David Talens-Perales, Julio Polaina, Identification and structural analysis of amino acid substitutions that increase the stability and activity of *Aspergillus niger* glucose oxidase, *PloS One*, 10, 12, (2015), 1-14 https://doi.org/10.1371/journal.pone.0144289

[17] Dušan Petrović, David Frank, Shina Caroline Lynn Kamerlin, Kurt Hoffmann, Birgit Strodel, Shuffling active site substate populations affects catalytic activity: the case of glucose oxidase, *ACS Catalysis*, 7, 9, (2017), 6188-6197 https://doi.org/10.1021/acscatal.7b01575

[18] Farhan Azhwin Maulana, Simulasi Termostabilitas Struktur Glukosa Oksidase *Aspergillus niger* IPBCC. 08.610 In-Silico, *Master Thesis*, Departement of Biochemistry, IPB University, Bogor, 2017

[19] Puspa Julistia Puspita, Laksmi Ambarsari, Adrian Adiva, Tony Ibnu Sumaryada, In Silico Analysis of Glucose Oxidase H516r and H516d Mutations for an Enzymatic Fuel Cell, *Jurnal Kimia Valensi*, 7, 2, (2021), 83-93 https://doi.org/10.15408/jkv.v7i2.20733

[20] Andrew Waterhouse, Martino Bertoni, Stefan Bienert, Gabriel Studer, Gerardo Tauriello, Rafal Gumienny, Florian T. Heer, Tjaart A. P. de Beer, Christine Rempfer, Lorenza Bordoli, SWISS-MODEL: homology modelling of protein structures and complexes, *Nucleic Acids Research*, 46, W1, (2018), W296-W303 https://doi.org/10.1093/nar/gky427

[21] Pilot Pipeline, in: Dassault Systèmes BIOVIA discovery studio modeling environment, In Release, 2016

[22] Zheng Yang, Keren Lasker, Dina Schneidman-Duhovny, Ben Webb, Conrad C. Huang, Eric F. Pettersen, Thomas D. Goddard, Elaine C. Meng, Andrej Sali, Thomas E. Ferrin, UCSF Chimera, MODELLER, and IMP: an integrated modeling system, *Journal of Structural Biology*, 179, 3, (2012), 269-278 https://doi.org/10.1016/j.jsb.2011.09.006

[23] Eric F. Pettersen, Thomas D. Goddard, Conrad C. Huang, Gregory S. Couch, Daniel M. Greenblatt, Elaine C. Meng, Thomas E. Ferrin, UCSF Chimera—a visualization system for exploratory research and analysis, *Journal of Computational Chemistry*, 25, 13, (2004), 1605-1612 https://doi.org/10.1002/jcc.20084

[24] Elmar Krieger, Keehyoung Joo, Jinwoo Lee, Jooyoung Lee, Srivatsan Raman, James Thompson, Mike Tyka, David Baker, Kevin Karplus, Improving physical realism, stereochemistry, and side-chain accuracy in homology modeling: Four approaches that performed well in CASP8, *Proteins: Structure, Function, and Bioinformatics*, 77, S9, (2009), 114-122 https://doi.org/10.1002/prot.22570

[25] Ch. Surendhar Reddy, K. Vijayasarathy, E. Srinivas, G. Madhavi Sastry, G. Narahari Sastry, Homology modeling of membrane proteins: a critical assessment, *Computational Biology and Chemistry*, 30, 2, (2006), 120-126 https://doi.org/10.1016/j.compbiolchem.2005.12.002

[26] Scott A. Hollingsworth, P. Andrew Karplus, A fresh look at the Ramachandran plot and the occurrence of standard structures in proteins, *BioMolecular Concepts*, 1, (2010), 271-283 https://doi.org/10.1515/bmc.2010.022

[27] Noel M. O'Boyle, Michael Banck, Craig A. James, Chris Morley, Tim Vandermeersch, Geoffrey R. Hutchison, Open Babel: An open chemical toolbox, *Journal of Cheminformatics*, 3, 1, (2011), 1-14 https://doi.org/10.1186/1758-2946-3-33

[28] Tom Hall, BioEdit: a user-friendly biological sequence alignment editor and analysis program for Windows 95/98/NT, *Nucleic Acids Symposium Series*, 1999

[29] Gita Syahputra, Simulasi docking kurkumin enol, bisdemetoksikurkumin dan analognya sebagai inhibitor enzim12-lipoksigenase, *Jurnal Biofisika*, 10, 1, (2014), 55-67

[30] Garrett M. Morris, Ruth Huey, William Lindstrom, Michel F. Sanner, Richard K. Belew, David S. Goodsell, Arthur J. Olson, AutoDock4 and AutoDockTools4: Automated docking with selective receptor flexibility, *Journal of Computational Chemistry*, 30, 16, (2009), 2785-2791 https://doi.org/10.1002/jcc.21256

[31] Roman A. Laskowski, Mark B. Swindells, LigPlot+: multiple ligand–protein interaction diagrams for drug discovery, *Journal of Chemical Information and Modeling*, 51, 10, (2011), 2778–2786 https://doi.org/10.1021/ci200227u

[32] Shuguang Yuan, H.C. Stephen Chan, Zhenquan Hu, Using PyMOL as a platform for computational drug design, *Wiley Interdisciplinary Reviews: Computational Molecular Science*, 7, 2, (2017), 1-10 https://doi.org/10.1002/wcms.1298

[33] Panagiotis L. Kastritis, Alexandre M.J.J. Bonvin, On the binding affinity of macromolecular interactions: daring to ask why proteins interact, *Journal of The Royal Society Interface*, 10, 79, (2013), 1-27 https://doi.org/10.1098/rsif.2012.0835

[34] Tareq Hameduh, Yazan Haddad, Vojtech Adam, Zbynek Heger, Homology modeling in the time of collective and artificial intelligence, *Computational and Structural Biotechnology Journal*, 18, (2020), 3494-3506 https://doi.org/10.1016/j.csbj.2020.11.007

[35] Jamal Raiyn, Anwar Rayan, How Much Sequence Identity Guarantee Good Models in Homology Modeling-Proteins from Serine Protease Family as a Test Case?, *International Conference on Bio-inspired Systems and Signal Processing*, 2009 https://doi.org/10.5220/0001379204550458

[36] Vincent B. Chen, W. Bryan Arendall, Jeffrey J. Headd, Daniel A. Keedy, Robert M. Immormino, Gary J. Kapral, Laura W. Murray, Jane S. Richardson, David C. Richardson, MolProbity: all-atom structure validation for macromolecular crystallography, *Acta Crystallographica Section D: Biological Crystallography*, 66, 1, (2010), 12-21 https://doi.org/10.1107/S0907444909042073

[37] Mallory R. Tollefson, Jacob M. Litman, Guowei Qi, Claire E. O'Connell, Matthew J. Wipfler, Robert J. Marini, Hernan V. Bernabe, William T.A. Tollefson, Terry A. Braun, Thomas L. Casavant, Structural insights into hearing loss genetics from polarizable protein repacking, *Biophysical Journal*, 117, 3, (2019), 602-612 https://doi.org/10.1016/j.bpj.2019.06.030

[38] Gabriel Studer, Christine Rempfer, Andrew M. Waterhouse, Rafal Gumienny, Juergen Haas, Torsten Schwede, QMEANDisCo—distance constraints applied on model quality estimation, *Bioinformatics*, 36, 6, (2020), 1765-1771 https://doi.org/10.1093/bioinformatics/btz828

[39] Marco Biasini, Stefan Bienert, Andrew Waterhouse, Konstantin Arnold, Gabriel Studer, Tobias Schmidt, Florian Kiefer, Tiziano Gallo Cassarino, Martino Bertoni, Lorenza Bordoli, SWISS-MODEL: modelling protein tertiary and quaternary structure using evolutionary information, *Nucleic Acids Research*, 42, W1, (2014), W252-W258 https://doi.org/10.1093/nar/gku340

[40] Pascal Benkert, Marco Biasini, Torsten Schwede, Toward the estimation of the absolute quality of individual protein structure models, *Bioinformatics*, 27, 3, (2011), 343-350 https://doi.org/10.1093/bioinformatics/btq662

[41] Peter I. Maxwell, Paul L.A. Popelier, Unfavorable regions in the ramachandran plot: Is it really steric hindrance? The interacting quantum atoms perspective, *Journal of Computational Chemistry*, 38, 29, (2017), 2459-2474 https://doi.org/10.1002/jcc.24904

[42] Andrio Suhadi, Rizarullah Rizarullah, Feriyani Feriyani, Simulasi docking senyawa aktif daun binahong sebagai inhibitor enzyme aldose reductase, *Sel Jurnal Penelitian Kesehatan*, 6, 2, (2019), 55-65 http://dx.doi.org/10.22435/sel.v6i2.1651

[43] Romain A. Studer, Benoit H. Dessailly, Christine A. Orengo, Residue mutations and their impact on protein structure and function: detecting beneficial and pathogenic changes, *Biochemical Journal*, 449, 3, (2013), 581-594 https://doi.org/10.1042/BJ20121221

[44] Richard M. Clark, Simon Tavaré, John Doebley, Estimating a nucleotide substitution rate for maize from polymorphism at a major domestication locus, *Molecular Biology and Evolution*, 22, 11, (2005), 2304-2312 https://doi.org/10.1093/molbev/msi228

[45] Michael Meyer, Gerd Wohlfahrt, Jörg Knäblein, Dietmar Schomburg, Aspects of the mechanism of catalysis of glucose oxidase: A docking, molecular mechanics and quantum chemical study, *Journal of Computer-Aided Molecular Design*, 12, 5, (1998), 425-440 https://doi.org/10.1023/A:1008020124326

[46] Rollando Rollando, Pendekatan Struktur Aktivitas dan Penambatan Molekul Senyawa 2-iminoethyl 2-(2-(1-hydroxypentan-2-yl) phenyl) acetate Hasil Isolasi Fungi Endofit Genus Fusarium sp pada Enzim β-ketoasil-ACP KasA Sintase dan Enzim Asam Mikolat Siklopropana Sintase, *Pharmaceutical Journal of Indonesia*, 3, 2, (2018), 45-51

[47] Mohammad Rizki Fadhil Pratama, Eko Suhartono, Understanding the Interaction Between Glutathione and Acetaminophen: A Docking Study Approach, *Dentino: Jurnal Kedokteran Gigi*, 3, 2, (2018), 215-219

[48] Gerd Wohlfahrt, Susanne Witt, Jörg Hendle, Dietmar Schomburg, Henryk M. Kalisz, H.-J. Hecht, 1.8 and 1.9 Å resolution structures of the *Penicillium amagasakiense* and *Aspergillus niger* glucose oxidases as a basis for modelling substrate complexes, *Acta Crystallographica Section D: Biological Crystallography*, 55, 5, (1999), 969-977 https://doi.org/10.1107/S0907444999003431

[49] Navid Nezafat, Zeinab Karimi, Mahboobeh Eslami, Milad Mohkam, Sanam Zandian, Younes Ghasemi, Designing an efficient multi-epitope peptide vaccine against *Vibrio cholerae via* combined immunoinformatics and protein interaction based approaches, *Computational Biology and Chemistry*, 62, (2016), 82-95 https://doi.org/10.1016/j.compbiolchem.2016.04.006

[50] Christopher C. Valley, Alessandro Cembran, Jason D. Perlmutter, Andrew K. Lewis, Nicholas P. Labello, Jiali Gao, Jonathan N. Sachs, The methionine-aromatic motif plays a unique role in stabilizing protein structure, *Journal of Biological Chemistry*, 287, 42, (2012), 34979-34991 https://doi.org/10.1074/jbc.M112.374504

[51] Qoonita Fadhilah, Daryono Hadi Tjahjono, Hubungan Kuantitatif Struktur dan Aktivitas Senyawa Turunan 3-Haloasilaminobenzoilurea sebagai Inhibitor Pembentukan Mikrotubulus, *Acta Pharmaceutica Indonesia*, 37, 3, (2012), 76-82

[52] Sandeep Kumar, Chung-Jung Tsai, Ruth Nussinov, Factors enhancing protein thermostability, *Protein Engineering, Design and Selection*, 13, 3, (2000), 179-191 https://doi.org/10.1093/protein/13.3.179

[53] Dipali Mhaindarkar, Raphael Gasper, Natalie Lupilov, Eckhard Hofmann, Lars I. Leichert, Loss of a conserved salt bridge in bacterial glycosyl hydrolase BgIM-G1 improves substrate binding in temperate environments, *Communications Biology*, 1, 1, (2018), 1-11 https://doi.org/10.1038/s42003-018-0167-7

[54] James B. Bassingthwaighte, Tamara M. Chinn, Reexamining Michaelis-Menten enzyme kinetics for xanthine oxidase, *Advances in Physiology Education*, 37, 1, (2013), 37-48 https://doi.org/10.1152/advan.00107.2012

[55] Zatta Yumni Ihdhar Syarafina, Mega Safithri, Maria Bintang, Rini Kurniasih, In Silico Screening of Cinnamon (Cinnamomum burmannii) Bioactive Compounds as Acetylcholinesterase Inhibitors, *Jurnal Kimia Sains dan Aplikasi*, 25, 3, (2022), 97-107 https://doi.org/10.14710/jksa.25.3.97-107